Journal
Cellular Neuroscience
and Oxidative Stress
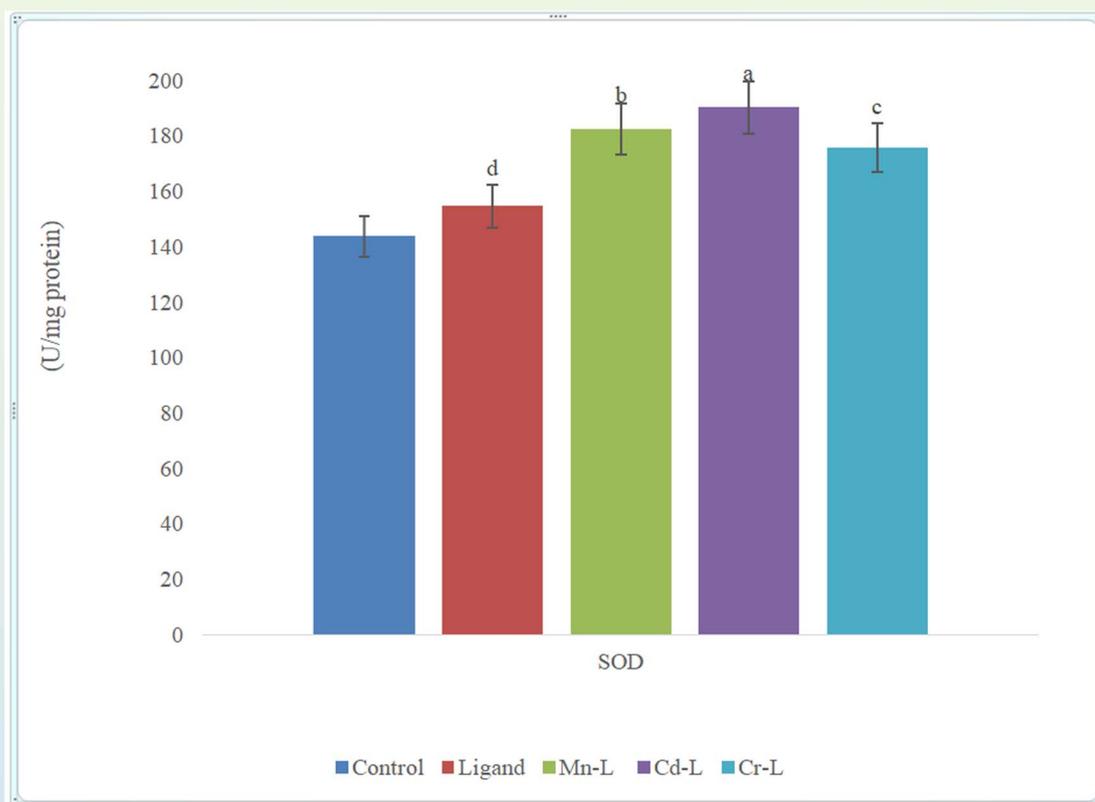
Editor in Chief
Prof.Dr. Mustafa NAZIROĞLU

Volume 11, Number 1, 2019

Journal of Cellular Neuroscience and Oxidative Stress

Volume 11, Number 1, 2019

[CONTENTS]

AIM AND SCOPES
Journal of Cellular Neuroscience and Oxidative Stress is an online journal that publishes original research articles, reviews and short reviews on the molecular basis of biophysical, physiological and pharmacological processes that regulate cellular function, and the control or alteration of these processes by the action of receptors, neurotransmitters, second messengers, cation, anions, drugs or disease.

Areas of particular interest are four topics. They are;

A- Ion Channels (Na^+- K^+ Channels, Cl^- channels, Ca^{2+} channels, ADP-Ribose and metabolism of NAD^+, Patch-Clamp applications)

B- Oxidative Stress (Antioxidant vitamins, antioxidant enzymes, metabolism of nitric oxide, oxidative stress, biophysics, biochemistry and physiology of free oxygen radicals)

C- Interaction Between Oxidative Stress and Ion Channels in Neuroscience
(Effects of the oxidative stress on the activation of the voltage sensitive cation channels, effect of ADP-Ribose and NAD^+ on activation of the cation channels which are sensitive to voltage, effect of the oxidative stress on activation of the TRP channels in neurodegenerative diseases such Parkinson's and Alzheimer's diseases)

D- Gene and Oxidative Stress
(Gene abnormalities. Interaction between gene and free radicals. Gene anomalies and iron. Role of radiation and cancer on gene polymorphism)

READERSHIP

Biophysics	Biochemistry
Biology	Biomedical Engineering
Pharmacology	PhysiologyGenetics
Cardiology	Neurology
Oncology	Psychiatry
Neuroscience	Neuropharmacology

Keywords
Ion channels, cell biochemistry, biophysics, calcium signaling, cellular function, cellular physiology, metabolism, apoptosis, lipid peroxidation, nitric oxide, ageing, antioxidants, neuropathy, traumatic brain injury, pain, spinal cord injury, Alzheimer's Disease, Parkinson's Disease.

Pregabalin protected cisplatin-induced oxidative neurotoxicity in neuronal cell line

Kemal ERTILAV

Departmant of Neurosurgery, Faculty of Medicine, Suleyman Demirel University, Isparta, Turkey

Abstract

Cisplatin (CSP) is used treatment of several cancers. However, it has also adverse effect through excessive reactive oxygen species production and activation of TRPV1 channel activation in neurons. Pregabalin (PGAB) has antioxidant and calcium channel blocker actions in neurons. I have investigated protective role of PGAB against the adverse effects of CSP in DBTRG neuronal cells.

*Author for correspondence :

Assist. Prof. Dr. Kemal Ertilav,

Department of Neurosurgery, Faculty of Medicine,

Suleyman Demirel University, Isparta, Turkey

Tel: +90 246 2112173

E-mail: drkertilav@gmail.com

List of Abbreviations;

AMG, [(E)-3-(4-t-butylphenyl)-N-(2,3-dihydrobenzo[b][1,4] dioxin-6-yl)acrylamide]; $[Ca^{2+}]_i$, cytosolic free Ca^{2+} ; Ca^{2+}, calcium ion; **Caps,** capsaicin; **Capz,** capsazepine; **CISP,** cisplatin; **DHR123**, dihydrorhodamine- 123; **GPx,** glutathione peroxidase; **GSH**, reduced glutathione; **JC1**, 5',6,6'-tetrachloro-1,1',3,3'-tetraethylbenzimi dazolylcarbocyanine iodide; **MTT,** 3-[4,5-Dimethyl-2-thiazolyl]-2,5-diphenyl- 2-tetrazolium bromide; **PGAB**, PGABalin; **PI**, propidium iodide; **ROS**, reactive oxygen species; **TRPV1**, transient receptor potential vanilloid 1

The neuronal cells were divided into four groups as control group, PGAB group (500 µM for 24 1 hrs), CSP group (25 µM for 24 hrs), and PGAB+CSP combination group. CISP-induced decrease of cell viability, glutathione peroxidase and glutathione level in the cells were increased in the neurons by PGAB treatment. However, CSP-induced increase of apoptosis, Ca^{2+} fluorescence intensity, TRPV1 current densities through the increase mitochondrial oxidative stress were decreased in the neurons by PGAB treatment. In conclusion, CSP-induced increases in mitochondrial ROS and cell death levels in the neuronal cells were decreased through the decrease of TRPV1 activation with the effect of PGAB treatment. CSP-induced drug resistance in the neurons might be reduced by PGAB treatment.

Introduction

Reactive oxygen species (ROS) occurs during the several physiological functions. Excessive ROS productions have adverse effects to membrane lipids, proteins and nucleic acids. Excessive ROS productions are scavenged by enzymatic and non-enzymatic antioxidants. For example, hydrogen peroxide is produced in cells by enzymatic action of superoxide dismutase and then it is converted to water by synergic actions between glutathione peroxidase (GPx) and reduced glutathione (GSH) (Schweizer et al., 2004). Most of chemotherapeutic agents kills tumors through excessive production of ROS in several cancers, but they have adverse effects to normal cells (Yakubov et al., 2014).

The Ca^{2+} controls several physiological and pathophysiological functions in neurons (Clapham, 2003). For example, development of a neuron needs Ca^{2+}, and excessive Ca^{2+} entry induces apoptosis in the neurons (Nazıroğlu, 2012). Cytosolic free $Ca^{2+}([Ca^{2+}]_i)$ concentration is increased in the cytosol through the activation of transient receptor potential (TRP) superfamily. The superfamily contains 6 subgroups in mammals, and one subgroup of the TRP superfamily is TRP vanilloid (TRPV) (Clapham, 2003; Ho et al., 2012). TRPV1 is a member of TRPV subgroup, and the channel is activated several stimuli including hot chili component (capsaicin, Caps), although its activity was inhibited by capsazepine (Capz) and AMG ([(E)-3-(4-t-butylphenyl)-N-(2,3-dihydrobenzo[b][1,4] dioxin-6-yl)acrylamide]) (Caterina et al., 1997; Gavva et al., 2005; Nazıroğlu, 2015).

Cisplatin (CSP) is common chemotherapeutic agent and it has been using several cancer such as brain tumors and breast cancer. CSP kills the tumor cells through activation or inhibition of several molecular pathways, including excessive production of reactive oxygen species (ROS) and overload entry of Ca^{2+} (Nazıroğlu and Braidy 2017; Xie et al., 2018). However, there is adverse effect CSP in neurons through the imbalance between CSP and excessive oxidative stress-induced overload calcium ion (Ca^{2+}) entry, although the adverse effects of CSP were treated by antioxidants (Piccolini et al. 2013; Chen et al. 2019; Popović et al. 2019).

Pregabalin (PGAB) is a voltage gated calcium channel (VGCC) blocker drug (Tomić et al. 2018). This drug also has been reported to show neuroprotective effects through its antioxidant role in rats (Al-Massri et al. 2018; Aslankoc et al. 2018). PGAB also inhibited the Ca^{2+} entry through inhibition of VGCC and TRPV1 channels in several neurons (Marwaha et al. 2016; Tomić et al. 2018). Hence, the PGAB may inhibit the TRPV1 channels in neurons. Accordingly, I presume that PGAB can potentiate the neurotoxicity effects of CSP through the inhibition of TRPV1 channel, and the subjects should be investigated for DBTRG neuronal cells.

I aimed to investigate the protective effects of PGAB against CSP-induced the adverse neurotoxicity and TRPV1 channel activation in the DBTRG cell line.

Materials and methods

Cell culture

In the current study I used DBTRG cell line because of presence TRPV1 channel in the cells. (Nazıroğlu et al., 2019). 90% of Dulbecco's modified Eagle's medium (DMEM, Invitrogen, Istanbul, Turkey) was used for growing the cells. Remaining 10% of the medium was fetal bovine serum (FBS, Gibco, Istanbul, Turkey). The cells were kept in a humidified atmosphere in 5% CO_2 at 37°C. Casy Modell TT model automatic cell counter (Roche, Germany) was used for counting the cells.

Groups

The DBTRG cells were mainly divided into four groups as follows;

Control (Ctr) group: The cells were kept in a flask containing the same cell culture medium and conditions for 26 hours without Caps, AMG, CSP and PGAB treatments.

PGAB group: After 2 hours pre-incubation of PGAB (500 µM) for two hours, the cells were kept in the cell culture conditions for 24 hours (Marmolino and Manto, 2010).

CSP groups: After keeping two hours in the cell culture medium, the cells in the group were incubated with CSP (25 µM) for 24 hours (Sakallı Çetin et al. 2017).

PGAB+CSP group: After incubating PGAB (500 µM) for two hours, the cells were further incubated with CSP (25 µM) for 24 hours.
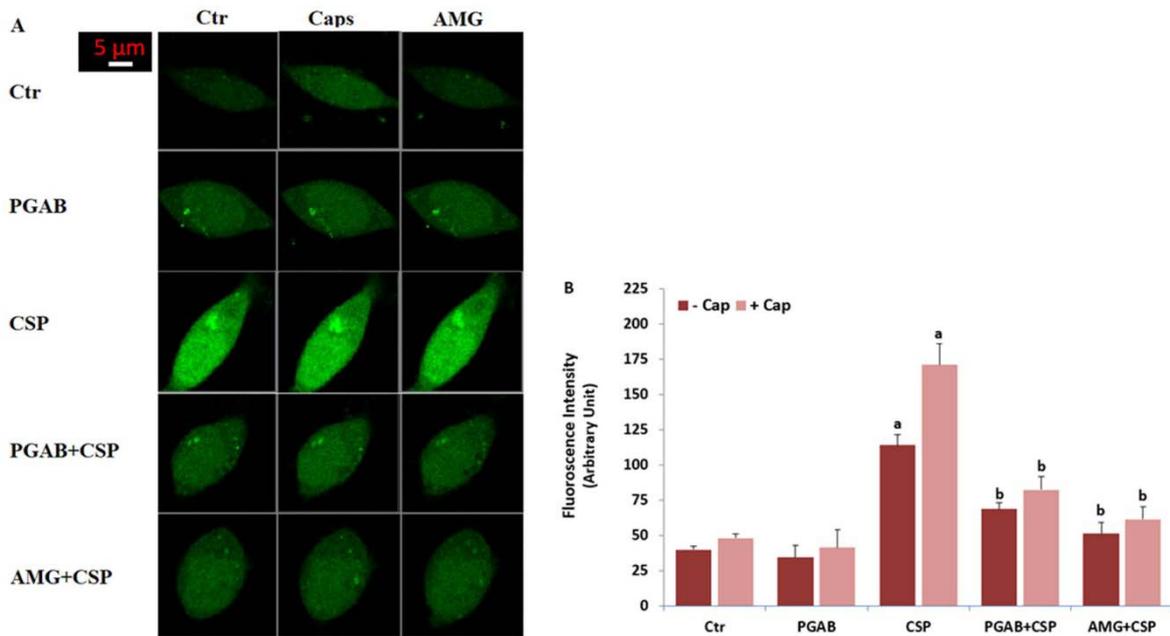
Figure 1. Effects of PGAB (500 µM) on the cisplatin (CSP)-induced increase of $[Ca^{2+}]_i$ levels in the DBTRG cells (mean ± SD). The cells in TRPV1 experiments are stimulated by Caps (10 µM for 5-10 min), but they were inhibited by AMG (10 µM for 5-10 min). Representative images of the effect of PGAB and CSP on the $[Ca^{2+}]_i$ levels through TRPV1 (Figure 1A) in the confocal microscope analyses. Changes of intensity of the $[Ca^{2+}]_i$ levels were shown by columns (Figure 1B). The scale bar = 5 µm. Objective: 40x oil. One example of each figure was taken from 6 independent experiments, with each experiment examining 20 cells for each condition ([a]$p \leq 0.001$ versus control (Ctr). [b]$p \leq 0.001$ versus CSP group).
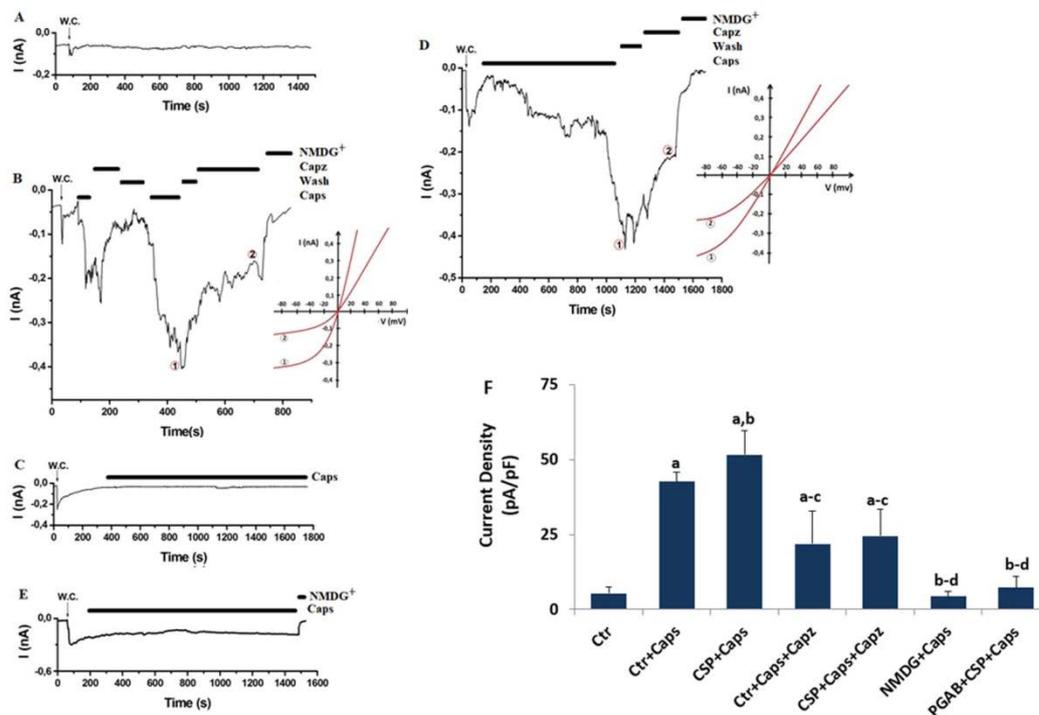
Figure 2. Effect of PGAB (500 µM) on the CSP-induced increase of TRPV1 current densities in the DBTRG cells (mean ± SD and n=3). The cells in TRPV1 experiments are stimulated by Caps (10 µM), but they were inhibited by Capz (0.1 mM). W.C. is whole cell. **A.** Ctr: Original recordings from control neuron. **B.** Caps group (without PGAB and CSP treatment). **C.** PGAB group without CSP treatment. **D.** CSP group without PGAB treatment. **E.** PGAB+CSP group. **F**. Representative images of the effect of PGAB and CSP on the current densities of TRPV1 channel. ([a]$p \leq 0.001$ versus control (Ctr). [b]$p \leq 0.001$ versus Ctr+Caps group. [c]$p \leq 0.001$ versus CSP+Caps group. [d]$p \leq 0.001$ versus Ctr+Caps+Capz and CSP+Caps+Capz groups).

The Caps, Capz, AMG, CSP and PGAB were purchased from Sigma-Aldrich Inc, (Istanbul, Turkey). Stock solutions of Cap, Capz, AMG and CSP were dissolved in DMSO (1%). PGAB was dissolved in sterile serum physiologic solution. Caps activated TRPV1 channel in the cell, but AMG and Capz blocked it.

Measurement of cytosolic free calcium ion ($[Ca^{2+}]_i$) concentration in laser confocal microscope

Incubation of 1 µM $[Ca^{2+}]_i$ indicator florescent dye (Fluo-3, Calbiochem, Darmstadt, Germany) was used in the cells for determining florescence intensity of the $[Ca^{2+}]_i$ concentrations (Ataizi et al. 2019). The Fluo-3 is a single wavelength excitation and emission dye that excited in a laser confocal microscopy (LSM 800, Zeiss, Ankara, Turkey) by a 488 nm argon laser. The cells were treated with TRPV1 antagonist AMG (10 µM) to inhibit Ca^{2+} entry before stimulation of Caps (10 µM).

Electrophysiology (patch-clamp analyses)

Whole-cell voltage clamp recording at room temperature was taken in EPC10 patch-clamp set (HEKA, Lamprecht, Germany) from the DBTRG cells. We used standard extracellular bath and pipette solutions as described in previous studies (Yüksel et al. 2017; Ataizi et al. 2019).

In the experiments, TRPV1 was extracellularly gated by Caps (10 µM), and the channels were extracellularly blocked by Capz (100 µM). The maximal current amplitudes (pA) in a DBTRG were divided by the cell capacitance (pF), a measure of the cell surface. Values of current density were expressed as pA/pF in the patch-clamp experiments.

Imaging of mitochondrial membrane depolarization (JC-1), mitochondrial and cytosolic ROS generation in the DBTRG cells by laser confocal microscope analyses

For the detection of mitochondrial membrane depolarization in the cells, JC-1 fluorescent dye was used (JC-1 (incubation with 5 µl JC-1 for 15 minutes at 37 °C in the dark). The samples were analyzed in a laser confocal microscopy (LSM 800, Zeiss, Ankara, Turkey) as described in previous studies (Joshi and Bakowska, 2011; Gökçe Kütük ve ark., 2019). The results of JC-1 were expressed as the mean fluorescence intensity in arbitrary unit /cell.

Mitochondrial ROS generation in the laser confocal microspore analyses (LSM 800) was assayed by using MitoTracker Red CM-H2Xros florescent dye according to manufacturer's instructions. Cytosolic ROS production was monitored by two fluorescent indicator dyes (DHR123 and DCFH-DA). After being exposed to these treatments, the cells were incubated in a culture medium containing 100 nM MitoTracker Red CM-H2Xros for 30 minutes, and 1 µM DCFH-DA or DHR123 for 20 minutes at 37 °C in dark (Keil et al., 2011; Gökçe Kütük et al. 2019).

Live (Hoechst)/ death (PI) analyses

For investigating death cells in laser confocal microscope (LSM 800) equipped with 20× objective, I used Hoechst 33342 (1 µM) and propidium iodide (PI and 5 µg/m) staining, respectively (Gökçe Kütük et al. 2019). The both dyes were bought from Cell Signaling Technology (Istanbul, Turkey). Cell death rate were expressed as %.

Image acquisition and analysis in the laser confocal microscope

Bride field and color images were collected with a LSM800 Zeiss inverted laser scanning confocal microscope. Fluorescence emissions of all analyses except PI/Hoechst in the cells were inspected with 40x oil objective on the laser confocal microscope and the analyses in the cells were taken from six independent experiments, with each experiment examining 25 cells for each. However, PI/Hoechst analyses in the cells were inspected with ultrafluar 20x (without oil) objective. Fluorescence intensity (arbitrary unit) of each cell as was recorded by using ZEN program and analyzed using ImageJ/Imaris software.

Assay of lipid peroxidation (LPx), reduced glutathione (GSH) level and glutathione peroxidase (GPx) activity

The levels of LPx (malondialdehyde, MDA), GSH and GPx in the DBTRG cells were spectrophotometrically (Cary 60 UV-Vis Spectrophotometer, Agilent, İzmir, Turkey) assayed at 512 nm and 412 nm by using the methods of Placer et al. (1966),
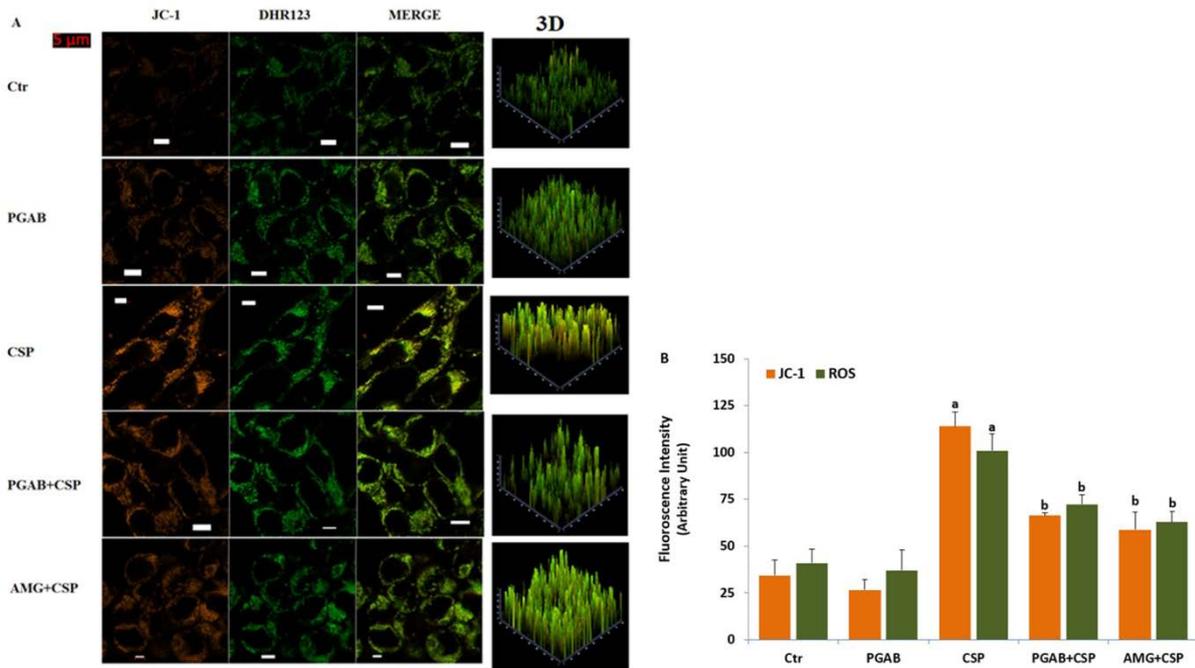
Figure 3. Effect of PGAB (500 µM) and CSP (25 µM) on the mitochondrial membrane depolarization (JC-1) and cytosolic ROS production (DHR123) levels in the cells (mean ± SD). The cells in TRPV1 experiments are stimulated by Caps (10 µM for 5-10 min), but they were inhibited by AMG (10 µM for 5-10 min). Representative color and 3D images of the effect of PGAB and CSP on the JC-1 and DHR123 (Figure 1A) in the confocal microscope analyses. Columns (Figure 1B) showed changes of intensity of the JC-1 and DHR123 levels. The scale bar = 5 µm. Objective: 40x oil. One example of each figure was taken from 6 independent experiments, with each experiment examining 20-25 cells for each condition ([a]p ≤ 0.001 versus control (Ctr) and PGAB groups. [b]p ≤ 0.001 versus CSP group).
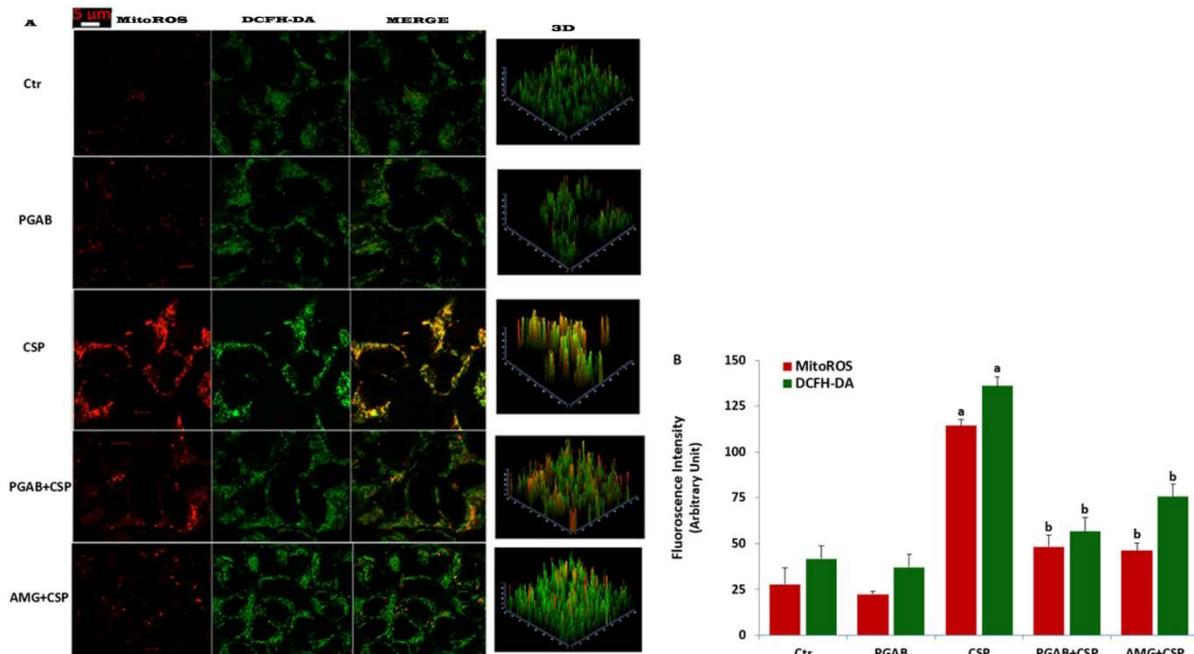
Figure 4. Effect of PGAB (500 µM) and CSP (25 µM) on the mitochondria (MitoROS) and cytosolic ROS production (DCFH-DA) levels in the cells (mean ± SD). The cells in TRPV1 experiments are stimulated by Caps (10 µM for 5-10 min), but they were inhibited by AMG (10 µM for 5-10 min). Representative images of the effect of PGAB and CSP on the MitoROS and DCFH-DA (Figure 1A) in the confocal microscope analyses. Columns (Figure 1B) showed changes of intensity of the MitoROS and DCFH-DA levels. The scale bar = 5 µm. Objective: 40x oil. One example of each figure was taken from 6 independent experiments, with each experiment examining 20 cells for each condition ([a]p ≤ 0.001 versus control (Ctr) and PGAB groups. [b]p ≤ 0.001 versus CSP group).

Sedlak and Lindsay (1968) and Lawrence and Burk (1976), respectively. LPx and GSH levels in cells were expressed as μmol/g protein, although GPx activity is expressed as an international unit (IU) of GSH oxidized/min/g protein. The total protein in the cells was spectrophotometrically (Shimadzu UV-1800) measured using the Lowry's method.

Statistical analyses

The values have been expressed in mean ± standard deviation (SD). Fisher's least significant difference (LSD) test was used in the four groups for determining statistical significance (SPSS program, version 18.0, software, SPSS. Chicago, IL, USA). The presence of statistical significance was detected as $p < 0.05$ by using a Mann-Whitney U test.

Results

CSP-induced increase of $[Ca^{2+}]_i$ florescence intensity was diminished though inhibition of TRPV1 by PGAB

In the current study, I investigated involvement of TRPV1 response to CSP treatment. The effects of the channels on $[Ca^{2+}]_i$ level were detected by detection of $[Ca^{2+}]_i$ levels using the TRPV1 (Caps) channel activator and blocker (AMG). In the results of the laser confocal microscope images (Figure 1A) and column (Figures 1B) of $[Ca^{2+}]_i$ fluorescence intensity levels of $[Ca^{2+}]_i$ was increased in CSP group by Caps stimulation (activation of TRPV1) ($p \leq 0.001$). The $[Ca^{2+}]_i$ fluorescence intensity levels was significantly ($p \leq 0.001$) lower in in the PGAB+CSP and AMG+CSP groups as compared to CSP only.

PGAB treatment diminished CSP-induced increase of TRPV1 current densities in the DBTRG cells

I observed Caps-induced increase of current density of TRPV1 channel in the patch-clamp experiments in the DBTRG. However, the current densities were reversibly blocked by Capz and $NMDG^+$ (replacement of Na^+). There were no currents in the absence of the Caps and Capz (Figure 2A). The current densities in the cells were significantly higher in the Ctr+Caps group (46.41 pA/pF) compared with the Ctr group (4.51 pA/pF) ($p \leq 0.001$) (Figure 2B); however, the current density was significantly ($p \leq 0.001$) lower

in the Ctr+Caps+Capz group (24.59 pA/pF) as compared to the Ctr+Caps group (46.41 pA/pF) (Figures 2B and 2F). The current densities in the cells were increased up to in 57.08 pA/pF in the CSP group (Figure 2D). There was no current and TRPV1 activation in the PGAB (2.72 pA/pF) and PGAB+CSP (4.97 pA/pF) groups by the Caps stimulation and they were significantly ($p \leq 0.001$) low in the PGAB and PGAB+CSP groups (Figures 2C, 2E and 2F). The present results indicated involvement of TRPV1 channel in the CSP-induced excessive Ca^{2+} entry and TRPV1 channel activation in the cells. However, the CSP-induced TRPV1 currents were decreased in the cells by the antioxidant PGAB treatment.

PGAB treatment diminished increase of CSP-induced mitochondrial membrane depolarization (JC1) and cytosolic ROS (DHR123) production levels in the neuronal cells

The electron transport system of mitochondria induces loss of mitochondrial membrane depolarization in the mitochondria (Joshi and Bakowska, 2011). For this reason, mitochondrial membrane depolarization is an important parameter of mitochondrial function and it was used as an indicator of normal cells. The laser confocal microscope analyses results of JC-1 and DHR123 levels are shown in Figure 3A. The JC1 and DHR123 fluorescence intensity were markedly ($p \leq 0.001$) higher in the CSP group than in the control and PGAB groups through Cap stimulations (activation of TRPV1) (Figure 3B). However, the JC1 and DHR123 levels were significantly ($p \leq 0.001$) decreased in the PGAB+CSP and AMG+CSP groups (inhibition of TRPV1) as compared to the CSP group.

PGAB diminished CSP-induced increase of mitochondrial (MitoROS) and cytosolic ROS (DCFH-DA) in the neuronal cells

The laser confocal microscope analyses results of MitoROS and DCFH-DA levels are shown in Figure 4. The MitoROS and DCFH-DA fluorescence intensity were markedly ($p \leq 0.001$) higher in the CSP group as compared to Ctr and PGAB groups through Cap stimulations (activation of TRPV1). However, the JC1 and DHR123 levels were significantly ($p \leq 0.001$) lower in the PGAB+CSP and AMG+CSP groups than in the CSP group.
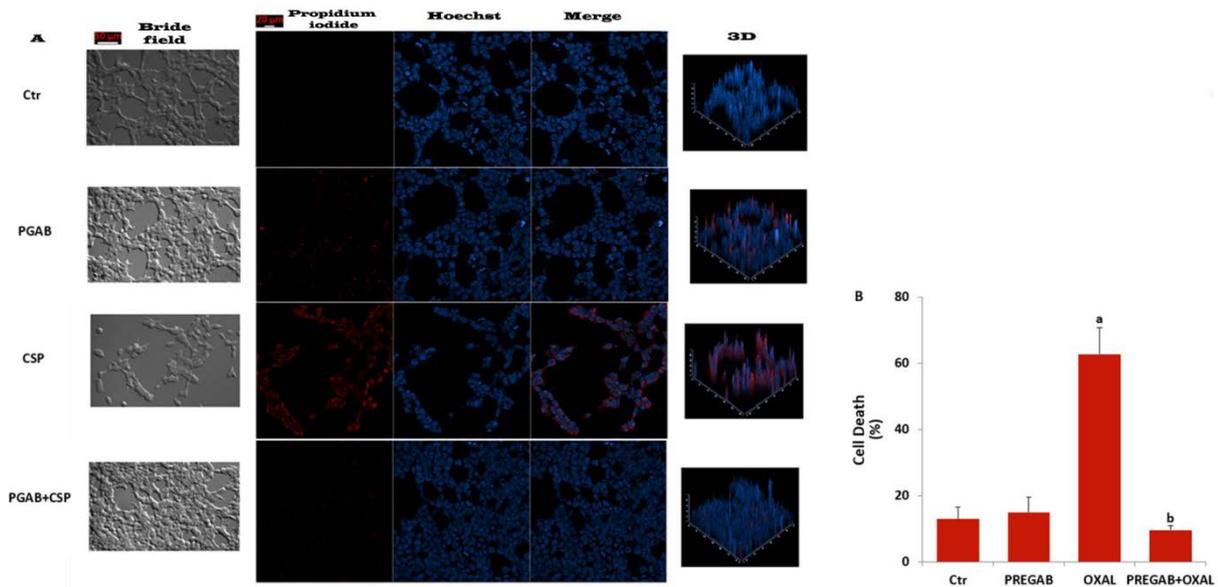
Figure 5. **PGAB (500 µM) protected CSP (25 µM)-induced cell death in the DBTRG cells. (mean ± SD). A.** Each panel consists of PI (red) and Hoechst (blue)-staining images are showing dead and live cells and merged Hoechst (blue)/PI (Merge) and 3D-staining image showing all and dead cells. The scale bar is 20 µm. **B.** Summary of the mean percentage of PI and Hoechst-positive cells under the indicated conditions from 6 independent experiments, with each experiment examining 20-25 cells for each condition ([a]$p \leq 0.001$ versus control (Ctr) and PGAB groups. [b]$p \leq 0.001$ versus CSP groups).
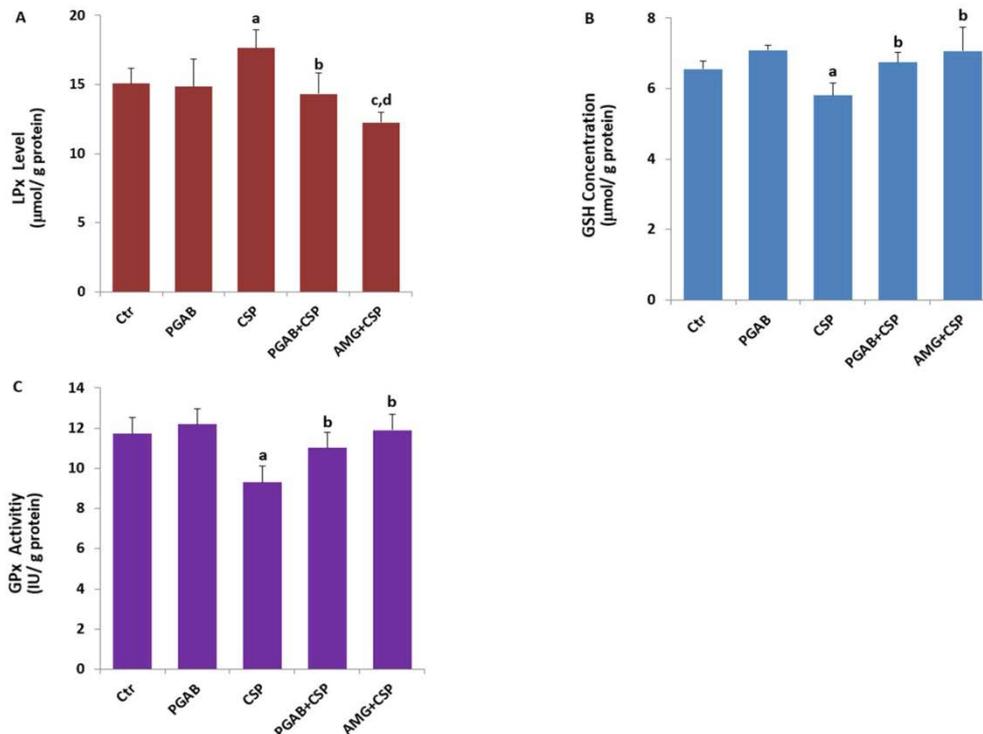

Figure 6. **PGAB (500 µM) protected CSP (25 µM)-induced lipid peroxidation (LPx) through increase of GPx activity and GSH level in the DBTRG cells. (mean ± SD and n=6).** The analyses were performed by the spectrophotometer. ([a]$p \leq 0.001$ versus control (Ctr) and PGAB groups. [b]$p \leq 0.001$ versus CSP group. [c]$p \leq 0.001$ versus PGAB+CSP group).

CSP-induced neuron death was diminished by the PGAB treatment

Accumulating evidences indicated that increase of $[Ca^{2+}]_i$ levels induces increase cell death levels through increase of mitochondrial ROS production. After observing the increase in mitochondria ROS and TRPV1 activation, we suspected whether cell death was increased in the DBTRG neurons. The percentage of dead cells was markedly ($p \leq 0.001$) higher in the CSP group than in the Ctr and PGAB groups (Figure 5A and B). However, PGAB induced cell protective action against the cell death and the percentage of dead cells was markedly ($p \leq 0.001$) lower in the PGAB+CSP group as compared the CSP group (Figure 5A and B).

CSP-induced LPx was diminished through increase of GSH and GPx in the neurons by the PGAB treatment

As oxidative stress played a key role on CSP-evoked neurotoxicity in the cells, we investigated whether PGAB pretreatments could improve CSP-induced LPx, GSH and GPx changes. As indicated in Figure 6A, B and C, CSP increased LPx levels, but its pre-treatment decreased the GSH levels and GPx activity in the cells. In contrast, treatment with PGAB in the cells improved the attenuated the levels of LPx, which rehabilitated the GSH and GPx ($p < 0.001$).

Discussion

In the current study, CSP-induced increase of apoptosis, cell death and mitochondria oxidative stress were acted through the TRPV1 activations resulting in the overload Ca^{2+} entry in the DBTRG neurons. However, we observed that antioxidant PGAB could protect the neuronal cells from CSP-caused oxidative injury through up-regulation of GSH and GPx, but downregulation of TRPV1 channel activity.

Platinum-induced peripheral neurotoxicity is a general adverse effect of platinum-based chemotherapy that may cause dose apoptosis and oxidative stress (Seto et al., 2019). The platinum-based chemotherapeutic agents including CSP mostly induce peripheral neurotoxicity in dorsal root ganglion (DRG) of spinal cord (Khasabova et al., 2019). Expression level of TRPV1 channel is high in the DRG neurons. Hence, it is a main responsible channel in the DRG neurons for management of CSP-induced peripheral neurotoxicity

(Nazıroğlu and Braidy, 2017). Results of recent studied indicated involvement of TRPV1 channel in the production of apoptosis and excessive mitochondria ROS production in the cancer cell treated with CSP and paclitaxel (Nur et al., 2017; Sakallı Çetin et al., 2017; Shim et al., 2019). In the current study, CSP induced activation of TRPV1 channels resulting in the overload Ca^{2+} entry in the DBTRG neurons. Hence, the results confirmed results of TRPV1 channel activation in the cancer cell treated with CSP and paclitaxel (Nur et al. 2017; Sakallı Çetin et al. 2017; Shim et al. 2019).

In the current study, we observed decrease of CSP-induced apoptosis, neuronal cell death mitochondrial membrane depolarization and ROS production through inhibition of TRPV1 in the DBTRG cells by PGAB treatment. Increase of mitochondria activation resulting in excessive ROS production is a side effect of CSP in neurons (Nazıroğlu and Braidy, 2017). Similarly, it was reported that the CSP-induced excessive mitochondria activation and ROS production was inhibited in the peripheral neurons by the antioxidant properties of PGAB, suggesting inhibition of excessive Ca^{2+} entry through membrane channel (TRPV1) (Sasaki et al. 2014; Marwaha et al. 2016). Decrease of CSP-induced neuropathy and neurotoxicity in the DRG neurons of rats was recently reported (Seto et al., 2017; Han et al. 2018) and the reports confirmed results of current study.

A major antioxidant in mammalian neurons is GSH. Several intracellular organelles such as endoplasmic reticulum, nuclei, and mitochondria contain high amount of GSH, although it is mostly synthetized in cytosol of body cells including neurons (Nam et al., 2018). It is well known that hydrogen peroxide and lipid hydroperoxide are scavenged in neurons by synergic actions between GPx and GSH (Schweizer et al., 2004). GSH homeostasis is important for the activation of TRPV1 channel and antioxidant treatments through upregulation of GSH concentrations in several neurons and cancer cells inhibited chemotherapeutic agent-induced TRPV1 activity (Nazıroğlu and Braidy 2017; Nur et al., 2017). In addition, TRPV1 channel was activated in neurons such as DRG and hippocampus by depletion of GSH, although it was inhibited in the neurons by cytosolic and extracellular GSH treatments (Nazıroğlu et al. 2013; Övey and Nazıroğlu, 2015). In the current study, CSP-

induced decreases of GSH concentration and GPx activity were increased in the neurons by the PGAB treatment, although LPx levels in the neuron decreased by the PGAB treatment. Similar to the current results, it was reported that CSP-induced neuropathic pain and oxidative stress were decreased through up-regulation of total antioxidant status in rats by the PGAB treatment (Al-Massri et al., 2018). Paclitaxel-induced increases of LPx, reduced glutathione (GSH), superoxide anion, calcium, myeloperoxidase (MPO) levels were decreased in sciatic nerve of mice by the PGAB treatment (Kaur and Muthuraman, 2019). Ischemia/reperfusion injury-induced decreases of GSH and GPx in the spinal cord neurons of rats were increased by PGAB treatment, although LPx levels were decreased in the samples by the treatment (Kazanci et al., 2017).

In conclusion, CSP caused neuronal cell death through up regulating Ca^{2+} entry and mitochondrial ROS production through activation of TRPV1 channel, but dwon regulating GSH and GPx values. However, PGAB protected the neurons through inhibition of the TRPV1 channel in the DBTRG cells. Hence, PGAB has potential neuroprotective actions against CSP induced neurotoxicity because of its antioxidant and TRPV1 channel blocker actions.

Acknowledgements

Conflict of interest declaration

The authors declare that there are no conflicts of interest.

References

Al-Massri KF, Ahmed LA, El-Abhar HS. (2018). Pregabalin and lacosamide ameliorate paclitaxel-induced peripheral neuropathy via inhibition of JAK/STAT signaling pathway and Notch-1 receptor. **Neurochem Internat** 120:164-171.

Aslankoc R, Savran M, Ozmen O, Asci S. (2018). Hippocampus and cerebellum damage in sepsis induced by lipopolysaccharide in aged rats - Pregabalin can prevent damage. Biomedicine and Pharmacotherapy 108:1384-1392.

Ataizi ZS, Ertilav K, Nazıroğlu M. (2019). Mitochondrial oxidative stress-induced brain and hippocampus apoptosis decrease through modulation of caspase activity, Ca(2+) influx and inflammatory cytokine molecular pathways in the docetaxel-treated mice by melatonin and selenium treatments. Metab Brain Dis. 34(4):1077-1089.

Caterina MJ, Schumacher MA, Tominaga M, Rosen TA, Levine JD, Julius D. (1997). The capsaicin receptor: a heat-activated ion channel in the pain pathway. Nature 389(6653):816-24.

Chen C, Zhang H, Xu H, Zheng Y, Wu T, Lian Y. (2019). Ginsenoside Rb1 ameliorates cisplatin-induced learning and memory impairments. J Ginseng Res. 43(4):499-507.

Clapham DE. (2003). TRP channels as cellular sensors. Nature 426(6966):517-524.

Gavva NR, Tamir R, Qu Y, Klionsky L, Zhang TJ, Immke D, Wang J, Zhu D, Vanderah TW, Porreca F, Doherty EM, Norman MH, Wild KD, Bannon AW, Louis JC, Treanor JJ. (2005). AMG 9810 [(E)-3-(4-t-butylphenyl)-N-(2,3-dihydrobenzo[b][1,4] dioxin-6-yl)acrylamide], a novel vanilloid receptor 1 (TRPV1) antagonist with antihyperalgesic properties. J Pharmacol Exp Ther. 313(1):474-484.

Gökçe Kütük S, Gökçe Kütük M, Gürses Cila HE, Nazıroğlu M. (2019). Curcumin enhances cisplatin-induced human laryngeal squamous cancer cell death through activation of TRPM2 channel and mitochondrial oxidative stress. Sci Rep 28;9(1):17784.

Han FY, Kuo A, Nicholson JR, Corradinni L, Smith MT. (2018). Comparative analgesic efficacy of pregabalin administered according to either a prevention protocol or an intervention protocol in rats with cisplatin-induced peripheral neuropathy. Clin Exp Pharmacol Physiol. 45(10):1067-1075.

Ho KW, Ward NJ, Calkins DJ. (2012). TRPV1: a stress response protein in the central nervous system. Am J Neurodegener Dis. 1(1):1-14.

Joshi DC, Bakowska JC. (2011). Determination of mitochondrial membrane potential and reactive oxygen species in live rat cortical neurons. J Vis Exp 51: 2704.

Kaur S, Muthuraman A. (2019). Ameliorative effect of gallic acid in paclitaxel-induced neuropathic pain in mice. Toxicol Rep 6:505-513.

Kazanci B, Ozdogan S, Kahveci R, Gokce EC, Yigitkanli K, Gokce A, Erdogan B. (2017). Neuroprotective effects of pregabalin against spinal cord ischemia-reperfusion injury in rats. Turk Neurosurg. 27(6):952-961.

Keil VC, Funke F, Zeug A, Schild D, Müller M. (2011). Ratiometric high-resolution imaging of JC-1 fluorescence reveals the subcellular heterogeneity of astrocytic mitochondria. Pflugers Arch. 462:693-708.

Khasabova IA, Khasabov SG, Olson JK, Uhelski ML, Kim AH, Albino-Ramírez AM, Wagner CL, Seybold VS, Simone DA. (2019). Pioglitazone, a PPARγ agonist, reduces cisplatin-evoked neuropathic pain by protecting against oxidative stress. Pain 160(3):688-701.

Lawrence RA, Burk RF. (1976). Glutathione peroxidase activity in selenium-deficient rat liver. Biochem Biophys Res Commun 71:952-958.

Marmolino D, Manto M. (2010). Pregabalin antagonizes copper-induced toxicity in the brain: in vitro and in vivo studies. Neurosignals 18(4):210-222.

Marwaha L, Bansal Y, Singh R, Saroj P, Sodhi RK, Kuhad A. (2016). Niflumic acid, a TRPV1 channel modulator, ameliorates stavudine-induced neuropathic pain. Inflammopharm. 24(6):319-334.

Nam E, Han J, Suh JM, Yi Y, Lim MH. (2018). Link of impaired metal ion homeostasis to mitochondrial dysfunction in neurons. Curr Opin Chem Biol. 43:8-14.

Nazıroğlu M, Braidy N. (2017). Thermo-sensitive TRP channels: Novel targets for treating chemotherapy-induced peripheral pain. Front Physiol. 8:1040.

Nazıroğlu M, Ciğ B, Ozgül C. (2013). Neuroprotection induced by N-acetylcysteine against cytosolic glutathione depletion-induced Ca2+ influx in dorsal root ganglion neurons of mice: role of TRPV1 channels. Neuroscience 242:151-160.

Nazıroğlu M. (2012). Molecular role of catalase on oxidative stress-induced Ca(2+) signaling and TRP cation channel activation in nervous system. J Recept Signal Transduct Res. 32(3):134-141.

Nazıroğlu M. (2015). TRPV1 channel: A potential drug target for treating epilepsy. Current Neuropharmacology 13:239-247.

Nur G, Nazıroğlu M, Deveci HA. (2017). Synergic prooxidant, apoptotic and TRPV1 channel activator effects of alpha-lipoic acid and cisplatin in MCF-7 breast cancer cells. J Recept Signal Transduct Res. 37(6):569-577.

Övey IS, Nazıroğlu M. (2015). Homocysteine and cytosolic GSH depletion induce apoptosis and oxidative toxicity through cytosolic calcium overload in the hippocampus of aged mice: involvement of TRPM2 and TRPV1 channels. Neuroscience 284:225-233.

Piccolini VM, Bottone MG, Bottiroli G, De Pascali SA, Fanizzi FP, Bernocchi G. (2013). Platinum drugs and neurotoxicity: effects on intracellular calcium homeostasis. Cell Biol Toxicol. 29(5):339-353.

Placer ZA, Cushman L, Johnson BC. (1966). Estimation of products of lipid peroxidation (malonyl dialdehyde) in biological fluids. Anal Biochem 16:359-364.

Popović J, Klajn A, Paunesku T, Ma Q, Chen S, Lai B, Stevanović M, Woloschak GE. (2019). Neuroprotective role of selected antioxidant agents in preventing cisplatin-induced damage of human neurons In Vitro. Cell Mol Neurobiol. 39(5):619-636.

Sakallı Çetin E, Nazıroğlu M, Çiğ B, Övey İS, Aslan Koşar P. (2017). Selenium potentiates the anticancer effect of cisplatin against oxidative stress and calcium ion signaling-induced intracellular toxicity in MCF-7 breast cancer cells: Involvement of the TRPV1 channel. J Recept Signal Transduct Res. 37:84-93.

Sasaki A, Mizoguchi S, Kagaya K, Shiro M, Sakai A, Andoh T, Kino Y, Taniguchi H, Saito Y, Takahata H, Kuraishi Y. (2014). A mouse model of peripheral postischemic dysesthesia:

involvement of reperfusion-induced oxidative stress and TRPA1 channel. J Pharm Sci. 351(3):568-575.

Schweizer U, Bräuer AU, Köhrle J, Nitsch R, Savaskan NE. (2004). Selenium and brain function: a poorly recognized liaison. Brain Res Brain Res Rev. 45(3):164-178.

Sedlak J, Lindsay RHC. (1968). Estimation of total, protein bound and non-protein sulfhydryl groups in tissue with Ellmann's reagent. Anal Biochem 25:192-205.

Seto Y, Takase M, Tsuji Y, To H. (2017). Pregabalin reduces cisplatin-induced mechanical allodynia in rats. J Pharmacol Sci. 134(3):175-180.

Shim HS, Bae C, Wang J, Lee KH, Hankerd KM, Kim HK, Chung JM, La JH. (2019). Peripheral and central oxidative stress in chemotherapy-induced neuropathic pain. Mol Pain 15:1744806919840098.

Staff NP, Cavaletti G, Islam B, Lustberg M, Psimaras D, Tamburin S. (2019). Platinum-induced peripheral neurotoxicity: From pathogenesis to treatment. J Peripher Nerv Syst 24 Suppl 2:S26-S39.

Tomić M, Pecikoza U, Micov A, Vučković S, Stepanović-Petrović R. (2018). Antiepileptic drugs as analgesics/adjuvants in inflammatory pain: current preclinical evidence. Pharm Ther 192:42-64.

Xie Q, Xu Y, Gao W, Zhang Y, Su J, Liu Y, Guo Y, Dou M, Hu K, Sun L. (2018). TAT-fused IP3R-derived peptide enhances cisplatin sensitivity of ovarian cancer cells by increasing ER Ca2+ release. Int J Mol Med. 41(2):809-817.

Yakubov E, Buchfelder M, Eyüpoglu IY, Savaskan NE. (2014). Selenium action in neuro-oncology. Biol Trace Elem Res. 161(3):246-254.

Yüksel E, Nazıroğlu M, Şahin M, Çiğ B. (2017). Involvement of TRPM2 and TRPV1 channels on hyperalgesia, apoptosis and oxidative stress in rat fibromyalgia model: Protective role of selenium. Sci Rep **7**(1):17543.